Materials Research. 2015; 18(2): 353-359
DOI: http://dx.doi.org/10.1590/1516-1439.315014

Structural and Mechanical Properties of Radiofrequency Ar-N_2 Plasma Nitrided Aluminium

Muhammad Hassan[a]*, Abdul Qayyum[b], Sarfraz Ahmad[b], Shahid Naseer[c], Noor Abbas Din Khattak[d], Muhammad Zakaullah[a]

[a]*Department of Physics, Quaid-i-Azam University, 45320 Islamabad, Pakistan*
[b]*National Tokamak Fusion Program, PO Box 3329 Islamabad, Pakistan*
[c]*Department of Physics, University of Peshawar, 25120 Peshawar, Pakistan*
[d]*Department of Physics, Gomal University, D.I. Khan, Pakistan*

Received: August 9, 2014; Revised: February 16, 2015

Aluminium (Al) samples were nitrided in 13.56 MHz radiofrequency (RF) discharge of 70:30 vol.% Ar:N_2 mixture at substrate temperature of 400 °C and RF power of 300 W for different fill pressures and treatment times. The nitrided samples were then characterized for their structural and mechanical properties using x-ray diffraction (XRD), scanning electron microscopy (SEM), energy dispersive x-ray spectroscopy (EDS), and Vickers micro hardness testing. XRD peaks (110), (111) and (200) of aluminium nitride (AlN) and their downshift confirmed the nitride formation together with nitrogen diffusion. The metastable cubic phase (c-AlN) shows texture growth and re-orientation dependent on fill pressure and treatment time. SEM micrographs showed the surface morphology with micro-pores. EDS results showed that the nitrogen content was significantly increased with nitriding time, along with the removal of oxides. Vickers hardness of the Al surface was increased more than thrice for 30 hours nitriding.

Keywords: *radiofrequency discharge, surface nitriding, structural and mechanical properties, surface hardness*

1. Introduction

Nitriding is a thermochemical process involving the deposition of nitride layer and the diffusion of nitrogen into metallic materials. The understanding and control of the nitride layer formation is of industrial interest owing to the improvement of surface properties such as resistance to wear, corrosion, and fatigue of metals and alloys[1,2]. AlN layers have attractive properties such as high hardness, electrical resistance and thermal conductivity[3,4]. AlN has been extensively investigated as a wide bandgap semiconductor material expected for many industrial applications such as short-wavelength light emitters, high-speed micro-electric devices, and surface acoustic devices[5,6]. A stable hexagonal phase (α-AlN) has a band gap of 6.2 eV, high chemical and thermal stability, electric resistance, and acoustic properties[7,8]. The metastable cubic-phase (c-AlN) is also attractive with a higher thermal conductivity, ballistic velocity, and acoustic velocity due to its better symmetry than α-AlN[9]. In addition, c-AlN films are expected as buffer layers for polarity control in the growth of semiconductor films such as GaN and ZnO[10]. However, the synthesis of c-AlN is more tricky than α-AlN[11,12]. Owing to fabrication difficulties of such films and experimental verifications, applications to industrial devices have poorly been implemented yet. Only the growth of ultra-thin films or small crystallites have been reported in recent past[10,13-15].

Plasma nitriding is one of the most favored methods having diversity in selecting process parameters including plasma composition, discharge frequency, fill pressure, input electrical power, substrate temperature and processing time. It is more economical and requires shorter treatment times and less gas consumption as compared to other commercial nitriding processes[3,4,16-18]. Plasma nitriding obviates the requirement of high temperature due to activation of plasma species responsible for nitriding. Therefore, there is an active ongoing research in the field of plasma nitriding of Al and its alloys[18-24]. A comprehensive description of plasma nitriding mechanisms is an extremely difficult task without understanding discharge and physiochemical characteristics of plasma, interaction of active nitrogen species with substrate surface and evolution of various phases in the nitrided layer. To achieve quality nitriding, it is essential to optimize the production of active species by a precise control on process parameters including input power, gas fill pressure, composition, substrate temperature, etc.[25,26]. For nitriding of metals, mixing of argon is advantageous regarding the enhancement and control of nitrogen active species concentration and consequent evolution of nitride growth[24,26,27].

*e-mail: hassanjh@gmail.com

In this communication, we report on nitriding of Al in Ar-N_2 mixture plasma energized by 13.56 MHz RF source and explore the influence of fill pressure and processing time on the microstructure, surface hardness and chemical composition in the nitrided layer. Particularly, the metastable AlN phase growth/re-orientation as a function processing time is investigated.

2. Experimental Setup

The Ar-N_2 mixture plasma was generated with 13.56 MHz 300 W RF source and commercially available polycrystalline Al (purity 99.4%) samples having 5mm×5mm×3mm dimensions were exposed for different fill pressures (0.1, 0.2, 0.3, 0.4 and 0.5 mbar), at fixed gas composition of 70 vol.% Ar in the mixture. The selection of this particular gas composition is based on early investigations of the same system by using optical emission spectroscopy (OES) for production and optimization of active species of nitrogen (N_2^+ and N) responsible for the plasma nitriding[26]. Prior to the treatment, the samples were mechanically polished by using different grit size silicon carbide papers and then mirror polished with 100 and 10 µm powder by using Metkon GRIPO 2V machine. The samples were ultrasonically cleaned in ethanol for 15 minutes and were placed on the bottom electrode for surface treatment. Prior to nitriding, the samples were cleaned for 20 minutes in Ar discharge at input power of 300 W and a pressure of 0.5 mbar in order to remove surface contaminants. To facilitate nitriding process, the samples were heated upto 400 °C temperature monitored by a thermocouple.

The samples were treated for 5 hours at 400 °C for various fill pressures in order to investigate the optimum pressure. Subsequent nitriding was accomplished at the optimum pressure of 0.5 mbar for various nitriding times (3, 6, 9… 30 hours) at fixed substrate temperature of 400 °C. The details of experimental set up are provided elsewhere[28]. The nitrided samples were analyzed by a JEOL JDX-3532 x-ray diffractometer (XRD) operated in detector scan mode at 40 kV, 30 mA using CuKα radiation (λ = 1.540598 Å). The surface morphology and elemental composition of the nitride layer were investigated by a Jeol-JSM-5910 scanning electron microscope (SEM) equipped with energy dispersive x-ray spectroscopy (EDS) attachment (INCA 200/ Oxford Instruments, U.K). The surface hardness was measured by using a Vickers micro hardness tester (Wilson Instrument 401 MVA) at applied loads of 10, 25, 50 and 100gf.

3. Results and Discussion

3.1. XRD analysis

Figure 1 presents the XRD spectra of the samples nitrided at different fill pressures (0.1, 0.2, 0.3, 0.4 & 0.5 mbar). The spectra show the diffraction peaks corresponding to c-AlN (110), (111) and (200) plane reflections respectively at 2θ positions of 32.05°, 38.92° and 45.50° (JCPD-ICDD database 00-046-1200). The insets (a) and (b) of Figure 1 show respectively typical (111) and (200) peaks of AlN. Al_2O_3 (012) peak was also observed at 25.54° in the spectrum of the sample nitrided at 0.4 mbar (JCPD-ICDD database 461212), which reports the possibility of significant production of active oxygen species under these conditions. The presence of oxygen content owes to the background air impurities at the working pressure as well as the native oxide layer on Al surface. The nitriding proceeds at a certain rate dictated by the removal of native oxide layer on the Al surface. However, the background air in the chamber supplies some oxygen content in parallel that re-oxides the Al. Both nitriding and oxidation take place with their rate depending upon the plasma conditions e.g. gas pressure, composition, substrate temperature, time etc. The effect of pressure on oxide removal and nitride formation is depicted by the presence of Al_2O_3 for 0.4 mbar. At this pressure electron energy distribution function is favorable for efficient oxygen active species production. The crystallinity of AlN (200) peak was maximum for the sample nitrided at 0.5 mbar pressure. It is well established that AlN formation is not the sole process during nitriding of Al owing to much less chemical affinity of nitrogen with Al. In addition to the compound formation, nitrogen diffusion occurs significantly at substrate temperature of 340 to 460 °C[29].

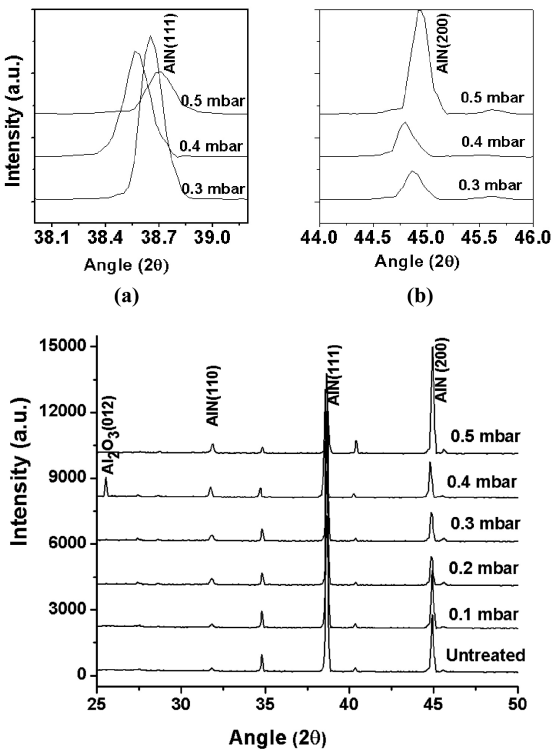

Figure 1. XRD spectra of Al samples nitrided at various filling pressures (0.1, 0.2, 0.3, 0.4 and 0.5 mbar) and fixed treatment time of 5 hours. Insets (a) and (b) resolve AlN(111) and (200) peaks.

The XRD spectra of the samples nitrided for various treatment times are shown in Figure 2. All the spectra show the appearance of (110), (111) and (200) diffraction peaks of c-AlN having lattice constant a = 4.0450Å. The diffraction peaks (110) and (111) of AlN seem to be merged with Al peaks owing to the very small difference in respective lattice parameters, and hence the peak positions. However, the peaks have been clearly resolved and exhibited in the insets (a) and (b) of Figure 2. The active N_2^+ species react chemically with

Al to form AlN along with nitrogen diffusion in the near surface region. We observe that AlN grows preferentially in (110) and (111) plane orientations for 12 hours and in (200) plane for 21 hours treatment. This can be associated with the optimum activation energy of AlN in a particular plane under these conditions. The metastable c-AlN phase evolves with plane orientations that change with the treatment time. Ogata et al.[18] investigated the crystalline orientation control of AlN films prepared by ion-beam-assisted technology as a function of ion energy.

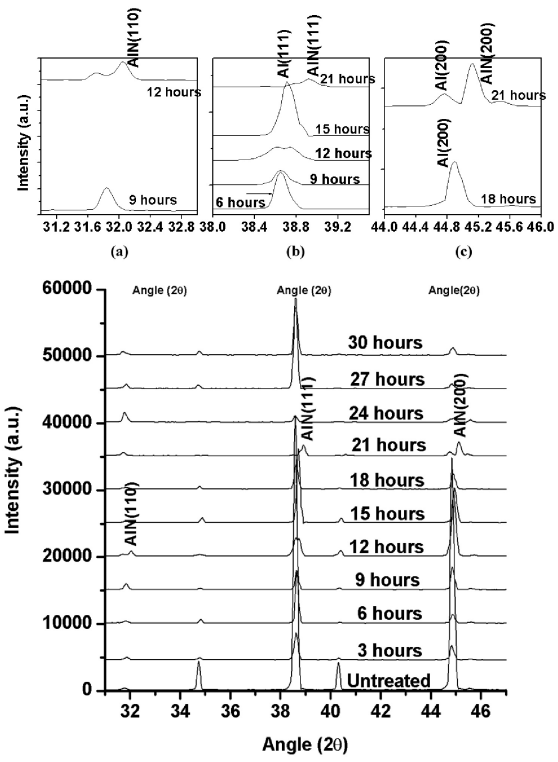

Figure 2. XRD spectra of Al samples nitrided at 0.5 mbar fill pressure for different treatment times (3, 6, 9, 12, 15, 18, 21, 24, 27 and 30 hours). Insets (a), (b) and (c) clearly resolve AlN(110) and (111) and (200) peaks.

The semi-quantitative analysis of the composition of AlN can be accomplished from the XRD peak intensities. The weight fraction of AlN in the sample surface W_{AlN} can be estimated using the following Formula 1[30]:

$$W_{AlN} = 1/ [1 + 0.884 (A_{Al}/A_{AlN})] \quad (1)$$

where A_{Al} and A_{AlN} represent the x-ray integrated intensities of Al and AlN peaks, respectively. It is observed that W_{AlN} varies from 0.59 to 0.88 respectively for 12 hours and 21 hours nitriding in (110) and (111) plane orientations when estimated against Al (111) plane. This is due to the texture re-orientation during nitriding process. The crystallite size of AlN is measured using the Scherrer's Formula 2:

$$\text{Crystallite size} = \frac{K\lambda}{\beta \cos\theta} \quad (2)$$

where $K = 0.99$ is the numerical constant, $\lambda = 1.540598$ Å is the x-ray wavelength, β is the broadening (in radians) of the diffraction peak and θ is the Bragg's angle. The variation of crystallite size of AlN estimated from a typical (110) plane at different fill pressures is shown in Figure 3a. With the increasing pressure, the crystallite size increases with a typical value of ~100 nm for 0.5 mbar pressure. This corresponds to a maximum N_2^+ active species predominantly responsible for AlN formation because the nitriding processes correlates with emission intensity of

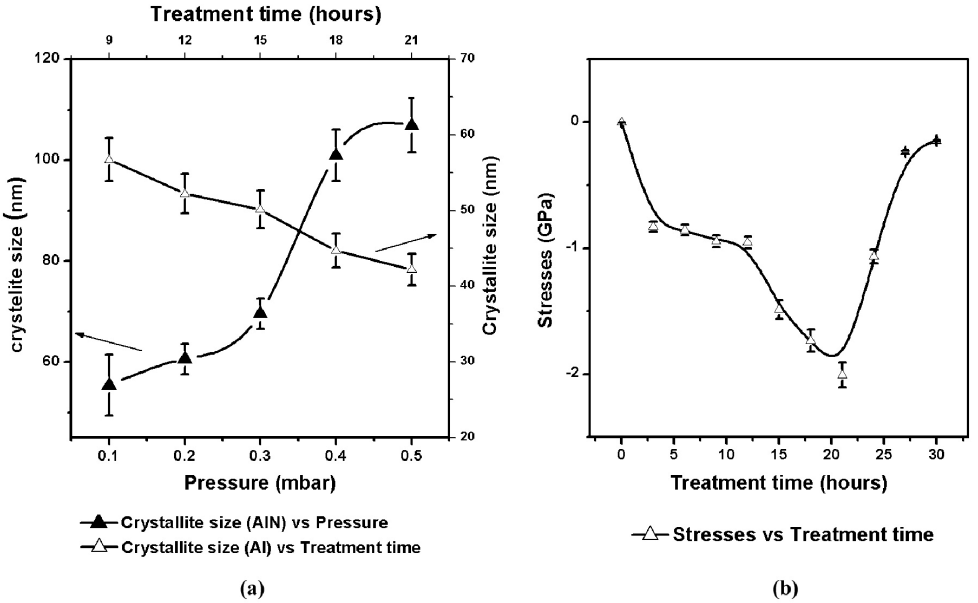

Figure 3. (a) Variation of crystallite size of AlN as a function of fill pressure (0.1, 0.2, 0.3, 0.4, 0.5 mbar) and treatment time (3, 6, 9…..30 hours), and (b) Variation of residual stresses in the substrate estimated from Al(111) plane as a function of treatment time (3, 6, 9, 12, 15, 18, 21, 24, 27 and 30 hours); all samples treated at 0.5 mbar fill pressure.

the first negative system of nitrogen N_2^+ [31]. The variation of crystallite size of Al matrix as a function of treatment time is also displayed in Figure 3a. A slight reduction in crystallite size of Al is caused due to stress incorporation by ion diffusion. Ion bombardment of noble gases also causes grain refinement and defects, as well as, increases the diffusion of active nitrogen species[32]. The diffusional transport during ion nitriding of Al is also accompanied by the diffusion of Al from the bulk to the surface that helps in AlN layer growth[33].

The rate of reaction in ion-nitriding can be enhanced by ion- or electron-impact-induced dissociation of physisorbed molecules[34] having a similar effect as the activation in the gas phase. During the reaction of low and medium energy ions (such as nitrogen) with solid surfaces[35] increasing the energy above a certain threshold leads to ion implantation i.e. nitrogen diffusion. Ochoa et al.[32] have investigated that noble gas bombardment generates stresses in the material. Moreover, nitrogen diffusion also produces stresses in the nitrided layer as well as in the near surface Al. We observe a shift in Al (111) peak having standard position at $2\theta = 38.50^o$. The down-shifting of peak indicates tensile stresses caused by diffusion of interstitial nitrogen into the Al lattice that generates lattice distortion. The stresses are generally tensile in nature and can be estimated by the Formula 3:

$$\text{Stresses} = \frac{E}{v}\left(\frac{d_{obs} - d_{sta}}{d_{sta}}\right) \quad (3)$$

where d_{OBS} and d_{STA} represent respectively the d-spacing (A˚) of the stressed and the stress-free diffraction planes parallel to the film surface. E is the Young's modulus and v is the Poison's ratio. Using the above expression, the tensile stress corresponding to strong Al (111) peak at 2θ=38.50^o varies from 0.83 GPa to 2.00 GPa by varying the treatment time and is presented in Figure 3b. It is observed that increasing treatment time initially increases tensile stresses, approaching maximum value (2.0 GPa) for 21 hours and then decreases again. This is explained by the fact that nitrogen diffusion interstitially causes texture re-orientation in the Al lattice as well as the nitride layer, leading to the phase growth in particular plane orientation depending upon the activation energy required. The texture re-orientation/phase growth is accompanied by the stress relaxation. The saturation of nitrogen diffusion for treatment time above 21 hours may be the reason of slight decrease in tensile stress.

All the diffraction peaks show broadening and shifting. The broadening increases with treatment time and approaches to the maximum value for 21 hours treatment, and then decreases owing to saturation of nitrogen diffusion accompanied by stress relaxation. The peak broadening not only reflects the crystallite size reduction but also includes the microstrain effect resulted by crystal defects[36].

3.2. SEM/EDS analysis

A visual examination reveals that the nitrided surfaces are dark grayish in color. Figure 4 provides the SEM micrographs of an untreated sample and samples nitrided for 3, 15, 21 and 30 hours. The surface of the untreated specimen (Figure 4a) appears smooth but having polishing marks. The surface of sample nitrided for 3 hours (Figure 4b) has sparsely distributed shallow ion impact craters/micropores formed due to nitrogen bombardment. The surfaces of sample nitrided for

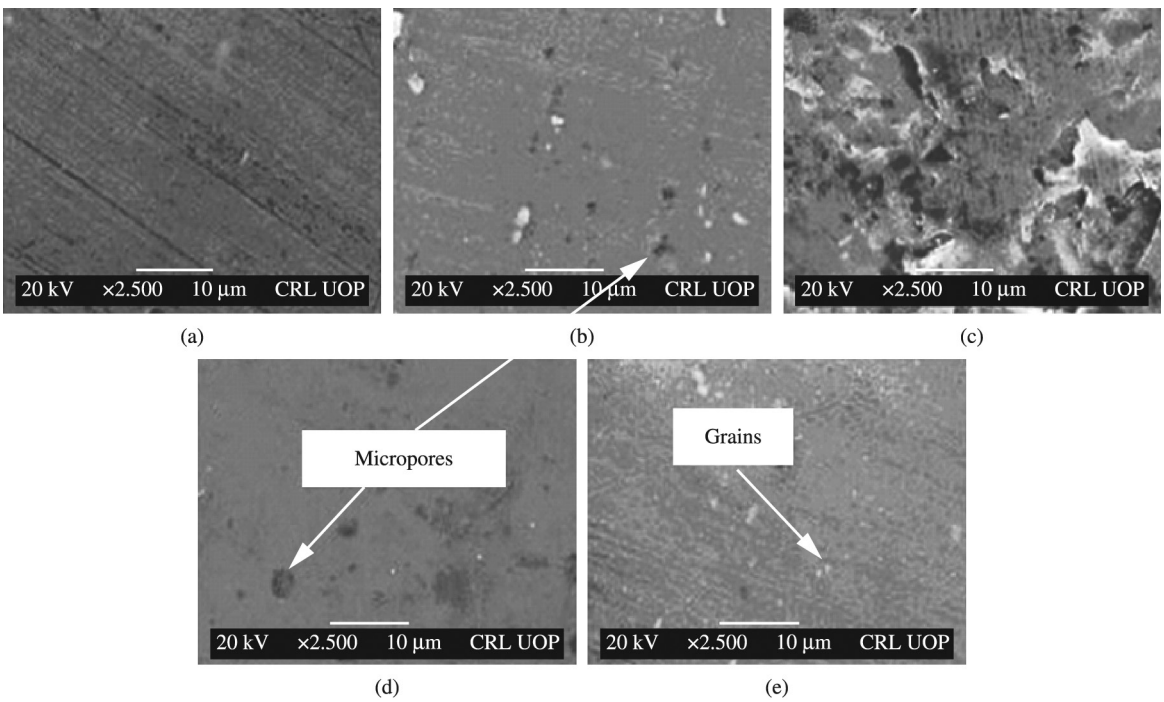

Figure 4. SEM micrographs of Al samples nitrided for different times at fill pressure of 0.5 mbar. (a) Untreated, (b) nitrided for 3 hours, (c) 15 hours, (d) 21 hours and (e) 30 hours.

time upto 12 hours (not shown) are found to exhibit similar morphology having micropores of almost identical size and distribution. Such micropores are resulted by the ion-induced impact, restructuring and defect migration during auxiliary heating of the substrate. However, for 15 hours treatment (Figure 4c), the surface is rough owing to significant surface damage by ions bombardment, but covered with shallow layer of nitride.

For 21 hours nitriding (Figure 4d), nitride layer grows with comparatively smooth surface but having some micropores. The spatial distribution of the micropores is, however, small and the layer appears denser. By increasing the nitriding time to 30 hours (Figure 4e), the nitride surface appears granular in nature. The micrograins have uniform dense spatial distribution, clearly patterning a continuous layer. The nitride pattering is accelerated with treatment time since the nitrogen diffusion in Al and the reaction rate of nitrogen with Al substrate at 400°C is significantly enhanced for higher treatment times having higher total density of active species. SEM investigations show that the processing time significantly affects the nitriding process, and eventually the surface morphology of the nitride layer.

The compositional analysis of the nitrided samples shows that nitrogen content gradually increases with nitriding time (from 3-30 hours). Table 1 provides the EDS data showing the variation of nitrogen and oxygen concentration with treatment time. For 3 hours nitriding, the oxygen content in the nitrided surface is reduced due to removal of oxides by ion bombardment. But the oxygen content again increases for 6 hours treatment due to enhanced oxidation in the plasma environment compared with the nitriding. However, by increasing processing time above 6 hours, the nitriding process overcomes the oxidation. Eventually, the nitride growth proceeds along with the oxide removal. This can be explained as follows: The nitriding process is accompanied by the oxidation natively present in the background environment. Even at a favorable discharge condition for nitriding i.e. 0.5 mbar pressure, the effect of oxidation due to background air cannot be eliminated for a certain time (9 hours in the present experiment). The nitride dominates oxidation initially upto 3 hours. However, for 6 hours treatment the substrate temperature is such that thermal energy of the plasma-substrate system facilitates poorly the oxide removal. But as the time increase (9 hours and above) further nitriding efficiently removes the oxides. It has been observed that the nitrogen and oxygen contents in the nitrided Al are strongly dependent on nitriding time.

3.3. Microhardness analysis

Figure 5 shows the variation of surface hardness of the samples nitrided for different treatment times at fill pressure of 0.5 mbar as a function of indentation depth. All the nitrided samples with increasing treatment time show an increase in surface hardness as compared to that of untreated one. The maximum surface hardness of 56 HV is estimated at the indentation depth of 1 μm for 30 hours nitriding. The enhanced surface hardness can be attributed to the formation of AlN compound and the nitrogen diffusion interstitially. It has also been strongly supported by the linear relationship between the hardness and nitrogen concentration investigated by Ochoa et al.[32]. It is obvious that up to ~2 μm depth, the surface hardness is doubled. Noticeably, the hardened zone also extends below the top layer owing to nitrogen diffusion. The surface hardness decreases with indentation depth and saturates below 4 μm depth.

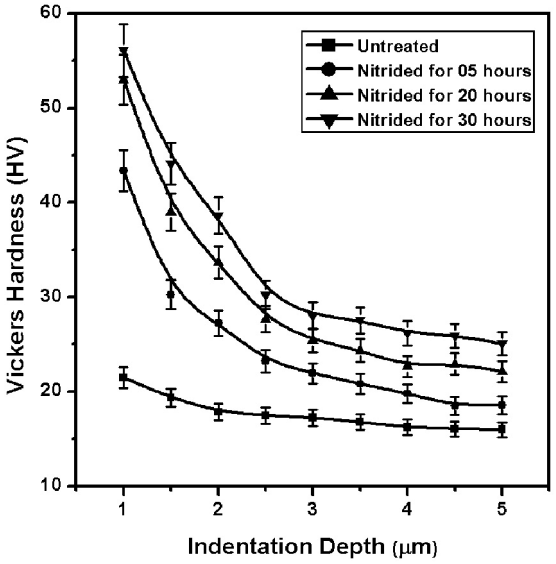

Figure 5. Variation of Vickers hardness as a function of indentation depth of samples nitrided for different times (15, 21 and 30 hours), at fill pressure of 0.5 mbar.

Table 1. Energy dispersive x-ray spectroscopy data showing the variation of nitrogen and oxygen content (at. % & wt. %) in samples nitrided for various treatment times at optimum fill pressure of 0.5 mbar.

Relative content	Treatment time (hours)									
	3 hrs	6 hrs	9 hrs	12 hrs	15 hrs	18 hrs	21 hrs	24 hrs	27 hrs	30 hrs
N (at.%)	4.99±0.99	6.64±1.32	10.1±2.02	12.97±2.59	13.39±2.67	15.8±3.16	16.08±3.21	19.99±3.99	21.92±4.38	22.76±4.55
N (wt.%)	3.99±0.79	4.31±0.86	8.78±1.75	8.98±1.79	11.48±2.29	11.88±2.37	12.2±2.44	11.48±2.29	13.37±2.67	13.59±2.71
O (at.%)	12.37±2.47	22.33±4.46	7.12±1.42	--	--	--	--	--	--	--
O (wt.%)	12.44±2.48	18.61±3.72	4.01±0.80	--	--	--	--	--	--	--

4. Conclusions

Plasma nitriding of Al samples at temperature of 400°C was performed in Ar-N_2 (70 vol.% Ar) 300 W RF plasma at various fill pressures and treatment times. The structural analysis of the nitrided Al samples confirmed AlN formation having (110), (111) and (200) plane reflections as well as nitrogen diffusion into the substrate surface. The crystallinity of AlN is maximum with the crystallite size of ~100 nm for nitriding at 0.5 mbar pressure. This is owing to the much efficient production of active nitrogen species. For 0.4 mbar, the formation of Al_2O_3 supersedes the nitriding process owing to the possibility of pronounced production of active oxygen species. The stress relieving occurs for nitriding above 21 hours. Nitrided samples depict smooth but micro-porous surface profile for lower treatment times (3-12 hours). For nitriding above 15 hours, the AlN layer smoothly grows with sparse micro-pores distributed on the surface. For higher treatment time, nitriding process dominates over oxidation. The metastable c-AlN shows texture growth and re-orientation dependent on fill pressure and treatment time. The surface hardness of nitrided Al has been increased more than thrice.

Acknowledgements

The authors express their gratitude and floral tributes to Faizullah Khan (Late) for his invaluable contributions and assistance in this research work. The authors acknowledge the financial support of the Higher Education Commission (HEC) Research Project No. 20-743(R & D) and Pakistan Science foundation Research Project No. PSF/Res/C-QU/Phy(138) for Plasma Physics Laboratory, Quaid-i-Azam University Islamabad, Pakistan.

References

1. Czerwiec T, Renevier N and Michel H. Low temperature plasma- assisted nitriding. *Surface and Coatings Technology*. 2000; 131(1-3):267-277. http://dx.doi.org/10.1016/S0257-8972(00)00792-1.
2. Venugupalan M. *Reactions under plasma conditions*. New York: Wiley-Interscience; 1971. v. 1.
3. Alsaran A and Celik A. Structural characterization of ion-nitrided AISI 5140 low-alloy steel. *Materials Characterization*. 2001; 47(3-4):207-213. http://dx.doi.org/10.1016/S1044-5803(01)00169-3.
4. Mondolfo LF. *Aluminium alloys: structure and properties*. Boston: Butterworths; 1976.
5. Taniyasu Y, Kasu M and Makimoto T. An aluminium nitride light-emitting diode with a wavelength of 210 nanometres. *Nature*. 2006; 441(7091):325-328. http://dx.doi.org/10.1038/nature04760. PMid:16710416
6. Kneissl M, Yang Z, Teepe M, Knollenberg C, Schmidt O, Kiesel P, et al. Ultraviolet semiconductor laser diodes on bulk AlN. *Journal of Applied Physics*. 2007; 101(12):123103. http://dx.doi.org/10.1063/1.2747546.
7. Li J, Nam KB, Nakarmi ML, Lin JY, Jiang HX, Carrier P, et al. Band structure and fundamental optical transitions in wurtzite AlN. *Applied Physics Letters*. 2003; 83(25):5163. http://dx.doi.org/10.1063/1.1633965.
8. Onuma T, Chichibu SF, Sota T, Asai K, Sumiya S, Shibata T, et al. Exciton spectra of an AlN epitaxial film on (0001) sapphire substrate grown by low-pressure metalorganic vapor phase epitaxy. *Applied Physics Letters*. 2002; 81(4):652. http://dx.doi.org/10.1063/1.1493666.
9. Petrov I, Mojab E, Powell RC, Greene JE, Hultman L and Sundgren JE. Synthesis of metastable epitaxial zinc blende structure AlN by solid state reaction. *Applied Physics Letters*. 1992; 60(20):2491. http://dx.doi.org/10.1063/1.106943.
10. Wang X, Tomita Y, Roh OH, Ohsugi M, Che SB, Ishitani Y, et al. Polarity control of ZnO films grown on nitride c-saphire by molecular-beam epitaxy. *Applied Physics Letters*. 2005; 86(1):011921. http://dx.doi.org/10.1063/1.1846951.
11. Wang LD and Kwok HS. Cubic aluminum nitride and gallium nitride thin films prepared by pulsed laser deposition. *Applied Surface Science*. 2000; 154-155:439-443. http://dx.doi.org/10.1016/S0169-4332(99)00372-4.
12. Shahien M, Yamada M, Yasui T and Fukumoto M. Cubic aluminum nitride coating through atmospheric reactive plasma nitriding. *J Therm Spray Technol*. 2010; 19(3):635-641. http://dx.doi.org/10.1007/s11666-010-9469-0.
13. Wang Y, Du XL, Mei ZX, Zeng ZQ, Ying MJ, Yuan HT, et al. Cubic nitridation layers on sapphire substrate and their role in polarity selection of ZnO films. *Applied Physics Letters*. 2005; 87(5):051901. http://dx.doi.org/10.1063/1.2001138.
14. Mikroulis S, Georgakilas A, Kostopoulos A, Cimalla V, Dimakis E and Komninou P. Control of the polarity of molecular beam epitaxy grown GaN thin films by the surface nitridation of Al2O3 (0001) substrates. *Applied Physics Letters*. 2002; 80(16):2886. http://dx.doi.org/10.1063/1.1472481.
15. Deng R, Muralt P and Gall D. Biaxial texture development in aluminum nitride layers during off-axis sputter deposition. *Journal of Vacuum Science & Technology. A, Vacuum, Surfaces, and Films*. 2012; 30(5):051501-1. http://dx.doi.org/10.1116/1.4732129.
16. Ogata K, Andoh Y and Fujimoto F. Role of ion beam energy for crystalline growth of thin films. *Nuclear Instruments & Methods in Physics Research. Section B, Beam Interactions with Materials and Atoms*. 1993; 80-81:1427-1430. http://dx.doi.org/10.1016/0168-583X(93)90814-M.
17. Hassan M, Ahmad R, Qayyum A, Murtaza G, Waheed A and Zakaullah M. Surface modification of AlFe1.8Zn0.8 alloy by using dense plasma focus. *Vacuum*. 2006; 81(3):291-298. http://dx.doi.org/10.1016/j.vacuum.2006.05.001.
18. Bouanis FZ, Bentiss F, Bellayer S, Vogt JB and Jama C. Radiofrequency cold plasma nitrided carbon steel: Microstructural and micromechanical characterizations. *Materials Chemistry and Physics*. 2011; 127(1-2):329-334. http://dx.doi.org/10.1016/j.matchemphys.2011.02.013.
19. Ogata K, Andoh Y, Sakai S and Fujimoto F. Crystalline orientation control for aluminum nitride films prepared by ion-beam-assisted technology. *Nuclear Instruments & Methods in Physics Research. Section B, Beam Interactions with Materials and Atoms*. 1991; 59-60:229-232. http://dx.doi.org/10.1016/0168-583X(91)95211-U.
20. Guzman L, Bonini G, Adami M, Ossi PM, Miotello A, Vittori-Antisari M, Serventi AM, Voltolini E. Mechanical behaviour of nitrogen-implanted aluminium alloys. *Surface and Coatings Technology*. 1996; 83:284-</jrn>289.
21. El-Hossary F, Negm NZ, Khalil SM and Raaif M. Effect of continuous and cyclic Rf plasma processing time on titanium

surface. *Applied Surface Science*. 2005; 239(2):142-153. http://dx.doi.org/10.1016/j.apsusc.2004.05.256.

22. Yamada M, Yasui T, Fukumoto M and Takahashi K. Nitridation of aluminum particles and formation process of aluminum nitride coatings by reactive RF plasma spraying. *Thin Solid Films*. 2007; 515(9):4166-4171. http://dx.doi.org/10.1016/j.tsf.2006.02.054.
23. Naseer S, Khan FU, Rehman NU, Qayyum A, Rahman F and Zakaullah M. Plasma nitriding of aluminium in a pulsed dc glow discharge of nitrogen. *The European Physical Journal Applied Physics*. 2010; 49(2):21001. http://dx.doi.org/10.1051/epjap/2009203.
24. Mayrhofer PM, Eisenmenger-Sittner C, Stöger-Pollach M, Euchner H, Bittner A and Schmid U. The impact of argon admixture on the c-axis oriented growth of direct current magnetron sputtered ScxAl1-xN thin films. *Journal of Applied Physics*. 2014; 115:193505-193508.
25. Wang Y, Chu PK, Tang BY, Zeng XC, Chen YB and Wang XF. Radio-frequency plasma nitriding and nitrogen plasma immersion ion implantation of Ti-6A1-4V alloy. *Surface and Coatings Technology*. 1997; 93:309-313.
26. Khan FU, Rehman NU, Naseer S, Naveed MA, Qayyum A, Khattak NAD, et al. Diagnostic of 13.56 MHz RF sustained Ar–N2 plasma by optical emission spectroscopy. *The European Physical Journal Applied Physics*. 2009; 45(1):11002. http://dx.doi.org/10.1051/epjap:2008198.
27. Tabbal M, Kazopoulo M, Chritidis T and Isber S. Enhancement of the molecular nitrogen dissociation levels by argon dilution in surface-wave-sustained plasmas. *Applied Physics Letters*. 2001; 78(15):2131-2133. http://dx.doi.org/10.1063/1.1359775.
28. Rehman NU, Zakaullah M, Khan FU and Naseer S. Characterization of nonthermal Ne–N2 mixture radio frequency discharge. *Journal of Applied Physics*. 2008; 104(12):123304-123309. http://dx.doi.org/10.1063/1.3021356.
29. Renevier N, Czerwiec T, Billard A, Von Stebut J and Michel H. A way to decrease the nitriding temperature of aluminium: the low-pressure arc-assisted nitriding process. *Surface and Coatings Technology*. 1999; 116-119:380-385.
30. Gribb AA and Banfield JF. Particle size effects on transformation kinetics and phase stability in nanocrystalline TiO2. *The American Mineralogist*. 1997; 82:717-728.
31. Walkowicz J, Supiot P, Smolik J and Grushin M. The influence of the N2-H2 mixture composition on the spectroscopic and temporal behaviour of glow discharge characteristics in pulse-supplied nitriding processes. *Surface and Coatings Technology*. 2004; 180-181:407-412.
32. Ochoa EA, Figueroa CA, Czerwiec T and Alvarez F. Enhanced nitrogen diffusion induced by atomic attrition. *Applied Physics Letters*. 2006; 88(25):254109. http://dx.doi.org/10.1063/1.2216032.
33. Telbizova T, Parascandola S, Kreissig U, Gunzel R and Moller W. Mechanism of diffusional transport during ion nitriding of aluminum. *Applied Physics Letters*. 2000; 76(11):1404-1406. http://dx.doi.org/10.1063/1.126070.
34. Utke I, Hoffmann P and Melngailis J. Gas-assisted focused electron beam and ion beam processing and fabrication. *Journal of Vacuum Science & Technology B Microelectronics and Nanometer Structures*. 2008; 26(4):1197-1276. http://dx.doi.org/10.1116/1.2955728.
35. Baldwin DA, Murray PT and Rabalais JW. Kinetic energy dependence of the reactions of N+ and N2+ with molybdenum. *Chemical Physics Letters*. 1981; 77(2):403-404. http://dx.doi.org/10.1016/0009-2614(81)80174-1.
36. Khan IA, Hassan M, Hussain T, Ahmad R, Zakaullah M and Rawat RS. Synthesis of nano-crystalline zirconium aluminium oxynitride (ZrAlON) composite films by dense plasma focus device. *Applied Surface Science*. 2009; 255(12):6132-6140. http://dx.doi.org/10.1016/j.apsusc.2009.01.066.